



## Human Cortical Neural Stem Cells Expressing Insulin-Like Growth Factor-I: A Novel Cellular Therapy for Alzheimer's Disease

LISA M. MCGINLEY,<sup>a</sup> ERIKA SIMS,<sup>a</sup> J. SIMON LUNN,<sup>a</sup> OSAMA N. KASHLAN,<sup>b</sup> KEVIN S. CHEN,<sup>b</sup> ELIZABETH S. BRUNO,<sup>a</sup> CRYSTAL M. PACUT,<sup>a</sup> TOM HAZEL,<sup>c</sup> KARL JOHE,<sup>c</sup> STACEY A. SAKOWSKI,<sup>d</sup> EVA L. FELDMAN<sup>a,d</sup>

**Key Words.** Neural stem cell • Insulin-like growth factor-I • Cellular therapy • Stem cell transplantation • Alzheimer's disease • Neurodegeneration

### ABSTRACT

Alzheimer's disease (AD) is the most prevalent age-related neurodegenerative disorder and a leading cause of dementia. Current treatment fails to modify underlying disease pathologies and very little progress has been made to develop effective drug treatments. Cellular therapies impact disease by multiple mechanisms, providing increased efficacy compared with traditional single-target approaches. In amyotrophic lateral sclerosis, we have shown that transplanted spinal neural stem cells (NSCs) integrate into the spinal cord, form synapses with the host, improve inflammation, and reduce disease-associated pathologies. Our current goal is to develop a similar "best in class" cellular therapy for AD. Here, we characterize a novel human cortex-derived NSC line modified to express insulin-like growth factor-I (IGF-I), HK532-IGF-I. Because IGF-I promotes neurogenesis and synaptogenesis *in vivo*, this enhanced NSC line offers additional environmental enrichment, enhanced neuroprotection, and a multifaceted approach to treating complex AD pathologies. We show that autocrine IGF-I production does not impact the cell secretome or normal cellular functions, including proliferation, migration, or maintenance of progenitor status. However, HK532-IGF-I cells preferentially differentiate into gamma-aminobutyric acid-ergic neurons, a subtype dysregulated in AD; produce increased vascular endothelial growth factor levels; and display an increased neuroprotective capacity *in vitro*. We also demonstrate that HK532-IGF-I cells survive peri-hippocampal transplantation in a murine AD model and exhibit long-term persistence in targeted brain areas. In conclusion, we believe that harnessing the benefits of cellular and IGF-I therapies together will provide the optimal therapeutic benefit to patients, and our findings support further preclinical development of HK532-IGF-I cells into a disease-modifying intervention for AD. *STEM CELLS TRANSLATIONAL MEDICINE* 2016;5:379–391

### SIGNIFICANCE

There is no cure for Alzheimer's disease (AD) and no means of prevention. Current drug treatments temporarily slow dementia symptoms but ultimately fail to alter disease course. Given the prevalence of AD and an increasingly aging population, alternative therapeutic strategies are necessary. Cellular therapies impact disease by multiple mechanisms, providing increased efficacy compared with traditional, single-target drug discovery approaches. This study describes a novel enhanced human stem cell line that produces increased amounts of growth factors beneficial to the disease environment. Findings support further development into a potentially safe and clinically translatable cellular therapy for patients with AD.

### INTRODUCTION

Alzheimer's disease (AD) is a progressive and irreversible neurodegenerative disorder, affecting an estimated 5.3 million people in the U.S. [1]. With increasingly aging populations and an unprecedented number of cases, AD is a significant public health concern; health-care costs exceeded \$200 billion in 2013 alone [1]. Patients typically exhibit progressive cognitive decline,

including memory loss and abnormalities in learning and behaviors, and the disease is ultimately fatal. Although the exact etiology and pathogenesis remain unclear, disease pathologies include amyloid  $\beta$  ( $A\beta$ ) plaques, hyperphosphorylated tau protein and neurofibrillary tangles [2–4], neuroinflammation, synapse loss, and massive neuronal damage across multiple regions [5, 6]. Current U.S. Food and Drug Administration (FDA)-approved drug treatments temporarily

<sup>a</sup>Department of Neurology, <sup>b</sup>Department of Neurosurgery, and <sup>d</sup>A. Alfred Taubman Medical Research Institute, University of Michigan, Ann Arbor, Michigan, USA; <sup>c</sup>Neuralstem, Inc., Germantown, Maryland, USA

Correspondence: Eva L. Feldman, M.D., Ph.D., 5017 AAT-BSRB, 109 Zina Pitcher Place, Ann Arbor, Michigan 48109, USA. Telephone: 734-763-7274; E-Mail: [efeldman@med.umich.edu](mailto:efeldman@med.umich.edu)

Received May 12, 2015; accepted for publication November 19, 2015; published Online First on January 7, 2016.

©AlphaMed Press  
1066-5099/2016/\$20.00/0

<http://dx.doi.org/10.5966/sctm.2015-0103>

slow dementia symptoms but fail to alter the course of the disease [7, 8]. Given the complexity of AD and the numerous pathways involved, it is increasingly likely that multifaceted approaches are necessary.

Cell-based therapies represent an entirely new approach to standard drug discovery and development pipelines because they impact disease by multiple mechanisms. In addition to tissue replacement, cellular therapy supports environmental enrichment through targeted and sustained delivery of paracrine factors [9]. A significant pathological finding in patients with AD is degeneration of neurons in areas connected to the cerebral cortex and hippocampus, particularly neurons in the basal forebrain and cholinergic neurons [10, 11]. These memory and learning centers of the brain are attractive targets for cellular therapeutics because impacting degeneration in these areas could potentially improve cognitive deficits in AD. Transplantation of neural stem cells (NSCs) to the hippocampal area improves cognition, neuronal survival, and synapse function in transgenic AD mice, mediated by NSC-derived neurotrophin activity [12–16]. Mesenchymal stem cells are also neuroprotective in AD through their ability to modulate cytokine levels and inflammation in the brain [17–19]. Many of these studies suggest that efficacy is enhanced when coupled with the delivery of trophic factors that can improve neurological disorders [20–22]. Combination approaches, in which stem cells are engineered to produce additional growth factors, provide increased cellular and trophic support [23–26]. Insulin-like growth factor-I (IGF-I) is an essential trophic factor for neuronal development and normal function [27, 28]. Signaling through the IGF-I receptor (IGF-IR) stimulates proliferation and differentiation [29–32], and exerts neuroprotective effects via activation of two major signaling pathways: the mitogen-activated protein kinase (MAPK) pathway and the phosphatidylinositol 3-kinase/Akt pathway [33, 34]. These neuroprotective effects are seen in multiple cell types, including cholinergic and hippocampal neurons [33, 35–37]. In vivo, IGF-I is antiapoptotic and anti-inflammatory, and promotes synapse formation [30, 31, 38–45]. Reduced IGF-I levels are associated with cognitive decline, and, conversely, increased IGF-I in the hippocampus prevents cognitive deficits [35, 46]. Thus, the neuroprotective capacity of IGF-I in degenerative disease and the correlation between decreased IGF-I and cognitive defects support the use of IGF-I in AD treatment approaches.

Our goal is to identify and develop a mechanism-based, “best in class” cellular therapy for patients with AD, and we anticipate that harnessing the benefits of cellular and growth factor therapies together will provide the required therapeutic option. In this study, we established the HK532-IGF-I cell line by modifying human cortical NSCs to produce increased IGF-I. We first characterized the effects of IGF-I production on normal NSC behaviors, including proliferation, migration, maintenance of progenitor status, and initial differentiation into selective neuronal subtypes. Next, we evaluated the therapeutic potential and neuroprotective capacity of HK532-IGF-I in an in vitro model of AD-associated A $\beta$ (1-42) toxicity. Importantly, we demonstrate in vivo engraftment and survival of HK532-IGF-I cells in the brain after peri-hippocampal transplantation in a mouse model of AD. Collectively, our findings strongly support further large-scale preclinical studies using transgenic models to determine the therapeutic efficacy of HK532-IGF-I cells as a disease-modifying treatment option for AD.

## MATERIALS AND METHODS

### HK532 Preparation, Culture, and Differentiation

The human cortical NSC lines (NSI-HK532 and NSI-HK532.UbC-IGF-I) were provided by Neuralstem, Inc. (Germantown, MD, <http://www.neuralstem.com>). Briefly, HK532 were prepared from cortical tissue obtained from a single 8-week-old human fetus following an elective abortion, as previously described [47, 48]. The material was donated to Neuralstem, Inc. with informed consent in a manner compliant with guidelines of the National Institutes of Health and the FDA, and according to guidelines that were reviewed and approved by an outside independent review board.

Cortical NSCs were conditionally immortalized using a retrovirus vector containing an immortalizing gene comprising human cMYC cDNA fused at the 3' end with a cDNA fragment coding for the c-terminal ligand binding domain of human estrogen receptor, and the neomycin-resistance gene. Cells were selected for neomycin resistance, propagated as a single cell line (HK532), and transduced with a replication-defective recombinant lentiviral vector to induce expression of human IGF-I, driven by the human ubiquitin C (UbC) promoter. Resulting cells were propagated as a single cell line without further selection (HK532.UbC-IGF-I).

HK532 and HK532-IGF-I cell lines were routinely cultured in Dulbecco's modified Eagle's medium (DMEM)/F12 (Corning, Manassas, VA, <http://www.cellgro.com>) supplemented with 10 ng/ml fibroblast growth factor (FGF) on poly-D-lysine (PDL), 100  $\mu$ g/ml, and fibronectin (FN), 25  $\mu$ g/ml, coated surfaces (Millipore, Billerica, MA, <http://www.emdmillipore.com>), according to our previously established NSC culture protocols [41, 42]. For differentiation, cells were cultured without FGF in differentiation medium (DMEM supplemented with 4 mM L-glutamine, 20  $\mu$ M L-alanine, 6  $\mu$ M L-asparagine, 67  $\mu$ M L-proline, 250 nM vitamin B<sub>12</sub>, 25 mg/l insulin, 100 mg/l transferrin, 20 nM progesterone, 100  $\mu$ M putrescine, and 30 nM sodium selenite), with 50% media changes every 2 days. Differentiated cell data are presented as days postdifferentiation (i.e., undifferentiated [D0], day 1 [D1], and so forth).

### Growth Factor Production and Signaling

IGF-I expression and signaling were determined by enzyme-linked immunosorbent (ELISA) and Western blotting, as previously described [33, 49]. To confirm IGF-I production and determine the NSC growth factor profile, conditioned medium was collected from D0, D3, and D7 cells, concentrated 10-fold to 1 ml using Centricon filters (3-kDa cutoff) (Millipore), and run on human-specific ELISAs for IGF-I (Assay Designs; Enzo Life Sciences Inc., Farmingdale, NY, <http://www.enzolifesciences.com>), brain-derived neurotrophic factor (BDNF), glial cell line-derived neurotrophic factor (GDNF), and vascular endothelial growth factor (VEGF) (all from Raybiotech, Norcross, GA, <http://www.raybiotech.com>), according to the manufacturer's instructions. For IGF-I signaling analysis, cells were cultured in differentiation medium without insulin for 4 hours before the addition of select inhibitors for 1 hour and subsequent addition of exogenous IGF-I (20 nM) for 30 minutes. Inhibitors included the Akt pathway inhibitor LY294002 (LY), 20  $\mu$ M (Sigma-Aldrich, St. Louis, MO, <https://www.sigmaaldrich.com>), the MAPK inhibitor U0126 (U), 20  $\mu$ M, (Millipore, La Jolla, CA, <https://www.emdmillipore.com>)

or the IGF-IR inhibitor NVP-AEW541 (NVP), 1  $\mu$ M (Sigma-Aldrich). For Western blot analysis, total cell protein was extracted in ice-cold radioimmunoprecipitation assay buffer (20 mM Tris; pH 7.4; 150 mM NaCl; 1 mM EDTA; 0.1% SDS; 1 mM Na deoxycholate; 1% Triton X-100; 0.1 trypsin units/l aprotinin, 10 mg/ml leupeptin, and 50 mg/ml phenylmethylsulfonyl fluoride), protein concentration was determined, and samples were electrophoresed on an sodium dodecyl sulfate polyacrylamide gel electrophoresis gel and transferred to nitrocellulose. Primary antibodies included phospho-IGF-IR (pIGF-IR), IGF-IR $\beta$  (Tyr1135/1136), phospho-Akt (Ser473) (pAkt), Akt, phospho-ERK (pERK), ERK (all from Cell Signaling Technology, Inc., Danvers, MA, <http://www.cellsignal.com>) and (Millipore, Temecula, CA, <http://www.emdmillipore.com>). After overnight primary antibody incubation at 4°C, membranes were incubated with the appropriate secondary antibody conjugated to horseradish peroxidase (Cell Signaling Technology) for 1 hour at 22°C, developed with a chemiluminescent substrate (SuperSignal West Pico; Thermo Fisher Scientific, Hampton, NH, <https://www.thermofisher.com>), and exposed to Kodak BioMax XAR film (Sigma-Aldrich).

### Cellular Migration

Undifferentiated HK532 and HK532-IGF-I cells were added to migration inserts following overnight storage at 4°C (1  $\times$  10<sup>6</sup> cells/ml or 3  $\times$  10<sup>6</sup> cells per vial), or were alternatively cultured on six-well plates and moved to inserts on D7 of differentiation. NSDM plus 10% fetal bovine serum was added below the inserts. After 24 hours, cells that had migrated through the insert were stained using the QCM 24-well Colorimetric Cell Migration Assay (Millipore). Migration was quantified using a standard LabSystems Fluoroskan Ascent FL microplate reader (Thermo Fisher Scientific) at 530 and 590 nm.

### Cellular Proliferation and Differentiation

Cellular proliferation and differentiation were assessed using standard immunocytochemistry (ICC) protocols [50, 51]. Briefly, HK532 and HK532-IGF-I cells were cultured on PDL/FN-coated glass coverslips. Proliferation was measured as previously described [51] at D0, D3, and D7 by incubating cells with 10  $\mu$ M 5'-ethynyl-2'-deoxyuridine (EdU) for 2 hours before fixation and processing following the manufacturers' protocols for the Click-It EdU kit (Thermo Fisher Scientific). EdU incorporation was measured by quantification of fluorescent images captured using an Olympus BX-51 microscope (Olympus Corp., Center Valley, PA, <http://www.olympusamerica.com>). Approximately 2.5  $\times$  10<sup>3</sup> to 2.7  $\times$  10<sup>3</sup> cells were counted per proliferation experiment for all samples ( $n = 3$ ).

To assess differentiation, cells were fixed with 4% paraformaldehyde (PFA), permeabilized with 0.1% Triton/phosphate-buffered saline (PBS), and blocked in 5% normal donkey serum per 0.1% Triton/PBS. Next, Ki67 (Novus Biologicals, Littleton, CO, <http://www.novusbio.com>), TUJ1 (Neuromics, Edina, MN, <http://www.neuromics.com>), Nestin (Millipore), glutamic acid decarboxylase 65/67 (GAD65/67) (Millipore), vesicular glutamate transporter 2 (VGLUT2) (Millipore), or IGF-IR $\beta$  (1:500; Sigma-Aldrich) primary antibodies were incubated at 1:1,000, unless otherwise indicated, overnight at 4°C. Cells were then incubated in Cy3, Cy5, or fluorescein isothiocyanate-conjugated secondary antibodies (Jackson ImmunoResearch, Westgrove, PA, <https://www.jacksonimmuno.com>) and mounted on glass slides using

ProLong Gold antifade with 4',6-diamidino-2-phenylindole (DAPI) (Thermo Fisher Scientific). Images were captured using an Olympus BX-51 microscope (Olympus Corp.) and approximately 2.5  $\times$  10<sup>3</sup> to 2.7  $\times$  10<sup>3</sup> cells were counted per differentiation experiment for all samples ( $n = 3$ ).

Maintenance of progenitor status and axonal outgrowth were assessed using our previously established neural index measurement [41, 42]. Briefly, cells were cultured on PDL/FN-coated glass coverslips for the first 7 days of differentiation and immunolabeled at D0, D3, and D7 with Nestin to identify neural progenitors, or with TUJ1 to observe primary neuronal processes. More than 2.5  $\times$  10<sup>3</sup> cells were counted per experiment for all Nestin-labeled samples ( $n = 3$ ). To calculate neural index, the number of neurons and neurite length were measured in TUJ1-labeled images using MetaMorph (Molecular Devices, Sunnyvale, CA, <http://www.moleculardevices.com>). Data are presented as neurite area per cell ( $\mu$ m<sup>2</sup> per cell) and a total of six images per condition were counted, representing approximately 7.5  $\times$  10<sup>3</sup> DAPI-labeled cells ( $n = 3$ ).

### Primary Cortical Neuron Preparation and Assessment of Neuroprotection

Primary cortical neurons (CNs) were isolated according to our previously published protocol [52]. Briefly, E15 Sprague-Dawley rat embryos were collected, membranes were removed, and the tissue was chopped into 2- to 3-mm pieces. Cells were dissociated by incubating the tissue in 0.5% trypsin/EDTA for 10 minutes at 37°C followed by trituration with a serum-coated glass pipette for 1 minute. The resulting cell suspension was applied to poly-L-lysine-coated glass coverslips (100  $\mu$ g/ml) in growth medium, which comprised Neurobasal Medium (Thermo Fisher Scientific) supplemented with 2.5 mg/ml albumin, 2.5  $\mu$ g/ml catalase, 2.5  $\mu$ g/ml superoxide dismutase, 0.01 mg/ml transferrin, 15  $\mu$ g/ml galactose, 6.3 ng/ml progesterone, 16  $\mu$ g/ml putrescine, 4 ng/ml selenium, 3 ng/ml  $\beta$ -estradiol, 4 ng/ml hydrocortisone, 1 $\times$  penicillin/streptomycin/neomycin, and 1 $\times$  B-27 additives (Thermo Fisher Scientific). To examine cell susceptibility to the toxic AD microenvironment, CN, HK532, and HK532-IGF-I cells (undifferentiated and D7 differentiated) were treated with 10  $\mu$ M A $\beta$ (1-42) (rPeptide, Bogart, GA, <https://www.rpeptide.com>) for approximately 72 hours. To assess NSC-mediated neuroprotective effects, primary CNs were cocultured with PDL/FN-coated, 3- $\mu$ m-pore transwell inserts (Corning) containing D7 HK532 or HK532-IGF-I. After 24 hours in NSDM, cocultures were starved overnight in treatment medium and subjected to 10  $\mu$ M A $\beta$  for 72 hours. The contribution of paracrine IGF-I production to protective capacity was assessed by adding 1  $\mu$ M NVP 2 hours before A $\beta$ . Cellular injury was determined by counting the percentage of cleaved caspase-3 (CC3)-positive cells following ICC with a CC3 antibody (1:1,000; Cell Signaling Technology). Approximately 3.0  $\times$  10<sup>3</sup> to 3.5  $\times$  10<sup>3</sup> cells were counted per neuroprotection experiment for all samples ( $n = 3$ ).

### In Vivo Transplantation

All procedures were in compliance with protocols approved by the University of Michigan (U-M) University Committee on Use and Care of Animals and detailed under protocol 3917. Daily monitoring and maintenance of mice was provided by the U-M Unit for Laboratory Animal Medicine. B6C3-Tg(APP<sup>swe</sup>/PSEN1 $\Delta$ E9)85Dbo/J (APP/PS1;  $n = 5$ ) and wild-type (WT) B6C3F1/J ( $n = 8$ )

mice were obtained from the Jackson Laboratory (Bar Harbor, ME, <https://www.jax.org>). At 11 weeks of age, mice received subcutaneous tacrolimus pellets (FK-506; Neuralstem, Inc.), which were continued for the study duration. At 12 weeks of age, mice were anesthetized with isoflurane and placed in a standard stereotactic frame (Stoelting Co., Wood Dale, IL, <http://www.stoeltingco.com>). HK532-IGF-I cell suspensions were administered by bilateral injections into the fimbria fornix of the hippocampus at three sites using the following coordinates from the bregma (axial, sagittal, and coronal planes):  $-0.82, 0.75, 2.5$ ;  $-1.46, 2.3, 2.9$ ; and  $-1.94, 2.8, 2.9$  mm, respectively, injecting a total cell number of 180,000 per animal. Two and 10 weeks after cell transplantation, animals were anesthetized and perfused with ice-cold saline, and their brains were dissected along the interhemispheric boundary and postfixed in 4% PFA overnight, followed by cryoprotection in 30% sucrose for immunohistochemistry (IHC).

Ten hippocampal sections ( $14 \mu\text{m}$ ) per animal were selected for IHC to detect grafted cells and verify accurate targeting to the fimbria fornix. Sections were rehydrated in PBS, permeabilized in 0.5% Triton X-100 in PBS for 20 minutes, and blocked in 5% donkey serum in 0.1% Triton X-100 in  $1\times$  PBS for 30 minutes. Primary antibodies for Doublecortin (DCX) and human nuclei (HuNu) (both from Millipore) were diluted 1:200 in blocking solution and incubated with sections overnight at  $4^{\circ}\text{C}$ . After primary antibody incubation, sections were washed three times in PBS and incubated for 1 hour with fluorescent-conjugated secondary antibodies raised in donkey (Alexa 488 and Alexa 594; 1:500; Thermo Fisher Scientific). Slides were mounted with glass coverslips using ProLong Gold antifade mounting medium containing DAPI nuclear stain (Thermo Fisher Scientific), and fluorescent images were captured using a Leica SP2 confocal microscope (Leica Microsystems, Buffalo Grove, IL, <http://www.leica-microsystems.com>).

### Statistical Analyses

All data are presented as mean  $\pm$  SD ( $n = 3$ ), or as representative images of three independent experiments. Statistical significance was determined by paired  $t$  tests or one-way analysis of variance followed by Tukey's multiple comparison test using GraphPad Prism (GraphPad Software Inc., La Jolla, CA, <http://www.graphpad.com>). Values of  $p < .05$  were considered statistically significant.

## RESULTS

### Growth Factor Production and Signaling

To enhance the efficacy of human cortex-derived HK532 cells as a cellular therapeutic, we generated the HK532-IGF-I cell line that stably produces IGF-I. ELISA analysis of conditioned medium demonstrated that parental HK532 cells produced very low to undetectable basal levels of IGF-I, whereas HK532-IGF-I cells produced 3–5 ng/ml of IGF-I between D0 and D7, approximately a 50-fold increase (Fig. 1A). Thus, HK532-IGF-I cells produced appreciable levels of IGF-I that were maintained throughout early differentiation, confirming robust and stable IGF-I expression. We also assessed the growth factor profile of the two cell lines by ELISA analysis on conditioned medium from undifferentiated and differentiated cells (Fig. 1D). BDNF and GDNF production did not considerably differ between cell lines

and time points, whereas VEGF production was significantly increased in undifferentiated HK532-IGF-I relative to parental cells.

Since NSCs respond to IGF-I signaling [41, 42, 53], we examined how growth factor receptor level and activation are regulated by autocrine IGF-I expression. By ICC, IGF-IR expression was observed along the cell surface of both parental HK532 and HK532-IGF-I cells at D7 (Fig. 1B, 1C). Western blot analysis confirmed this expression, which was significantly increased after differentiation in both cell lines (Fig. 1E). Although slightly reduced IGF-IR expression levels were observed in HK532-IGF-I cells relative to HK532 cells at D0 and D7, IGF-IR phosphorylation and signaling activation did not significantly differ between cell lines, and addition of exogenous IGF-I resulted in increased phosphorylation of the receptor (Fig. 1E) and was significantly more pronounced after differentiation.

We next assessed phosphorylation and downstream activation of MAPK/Akt pathways in HK532 and HK532-IGF-I cells (Fig. 1E). While basal MAPK signaling was present at D0 and D7, there were no significant differences between cell lines, and IGF-I stimulation only increased signaling after differentiation. Basal Akt signaling, however, was significantly increased in D0 HK532-IGF-I cells and in both cell lines after differentiation. Addition of exogenous IGF-I promoted a robust increase in Akt in HK532 cells after differentiation, whereas very little Akt activation was observed following IGF-I stimulation in HK532-IGF-I. These data demonstrate a decreased responsiveness of HK532-IGF-I to exogenous IGF-I relative to parental cells. Notably, inhibition of MAPK signaling increased Akt phosphorylation and inhibition of Akt signaling resulted in the reverse observation, suggesting that these pathways are capable of compensatory signaling. Inhibition of IGF-IR signaling using the receptor antagonist NVP did not affect MAPK signaling but significantly depleted activation of IGF-IR and Akt to below basal levels in both cell lines (Fig. 1E). Together, these data demonstrate that HK532-IGF-I cells exhibit normal IGF-IR and MAPK/Akt signaling profiles, albeit with an expected diminished responsiveness to exogenous IGF-I stimulation.

### IGF-I Expression Does Not Alter HK532 Proliferation or Migration

IGF-I can impact various cell behaviors, such as proliferation and migration [29, 32]; therefore, we next used EdU incorporation to assess the effect of IGF-I on HK532 and HK532-IGF-I cell proliferation. Approximately 36% and 33% of untreated D0 HK532 and HK532-IGF-I cells were EdU positive, respectively (Fig. 2A–2E). At D3, 6% and 9% of HK532 and HK532-IGF-I were EdU-positive, respectively, and by D7, less than 3% of either cell line was EdU positive. Thus, no differences in the proliferation profiles were observed at D0, D3, or D7, and both lines exhibited minimal proliferation at D7. These data demonstrate that IGF-I does not promote or maintain proliferation during the initial stages of differentiation. The effect of IGF-I on HK532 and HK532-IGF-I migration was also assessed at D0 and D7. Comparable migration levels were observed for HK532 and HK532-IGF-I at both time points tested (Fig. 2F, 2G). Furthermore, when additional IGF-I was added below transwell inserts, no change was detected (data not shown). Thus, induced IGF-I expression exerted no discernible effects on NSC migration.

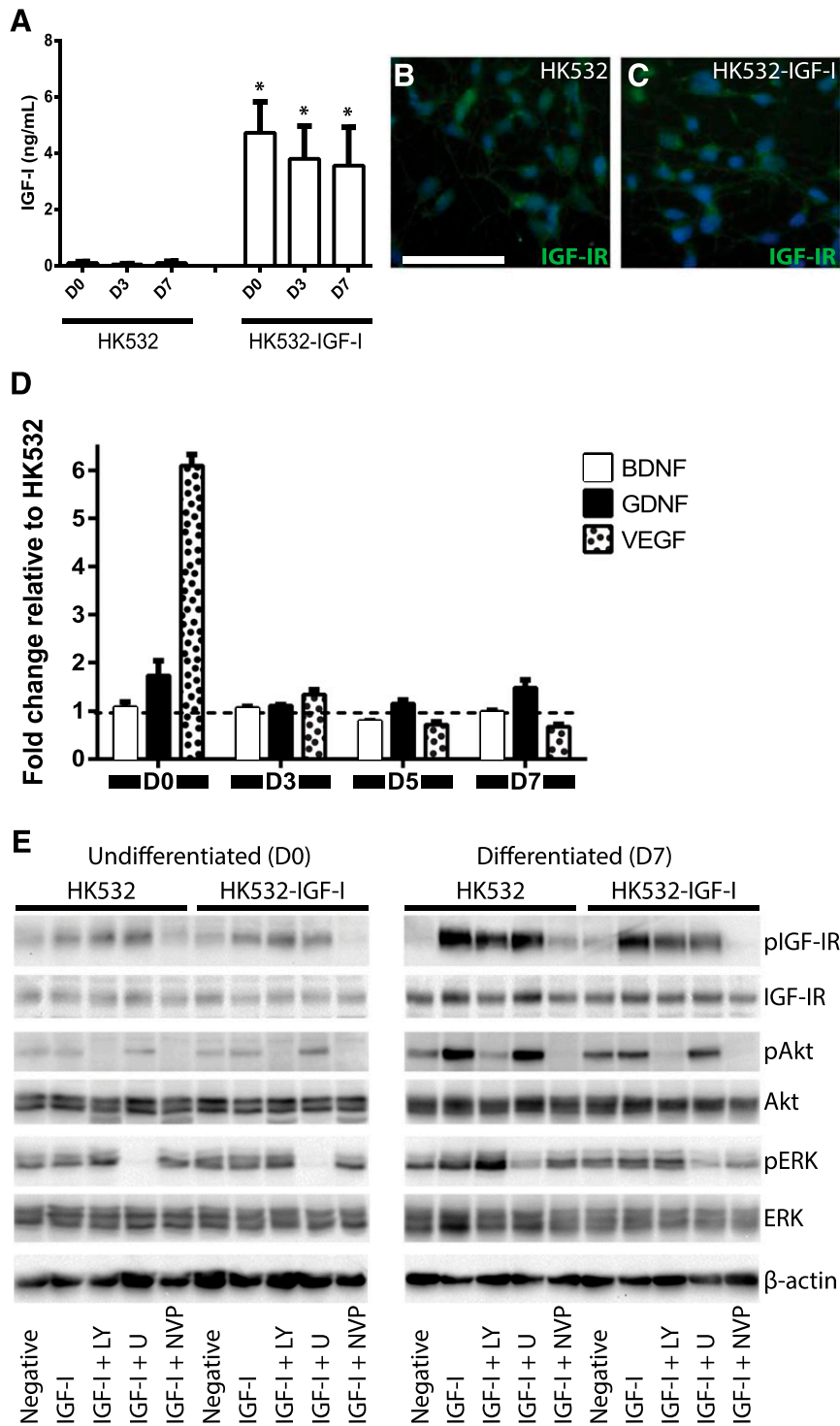


**Figure 1.** IGF-I production, growth factor profile, and signaling in HK532 and HK532-IGF-I cells. **(A):** Production of IGF-I in HK532 and HK532-IGF-I throughout early differentiation. Representative immunocytochemistry images of D7 HK532 **(B)** and HK532-IGF-I **(C)** cells labeled with 4',6-diamidino-2-phenylindole (DAPI) (blue) and IGF-IR (green). **(D):** BDNF, GDNF, and VEGF production in undifferentiated HK532 and HK532-IGF-I cells (D0) and throughout early differentiation (D3, D5, and D7). Growth factor production is expressed as fold change relative to parental HK532 cells. **(E):** Western blot analysis of IGF-I signaling in undifferentiated and differentiated (D7) HK532 and HK532-IGF-I cells. Cells were treated with an inhibitor panel of LY, U, or NVP for 1 hour, followed by IGF-I treatment for 30 minutes. All blots were probed with pIGF-IR, IGF-IR, pERK, ERK, pAKT, and AKT. β-actin was used as a loading control. Data are presented as mean + SD or are representative images of at least three independent experiments. Scale bar = 50 μm. \*, *p* < .05. Abbreviations: BDNF, brain-derived neurotrophic factor; D0 (D3, D7), day 0 (day 3, day 7); GDNF, glial cell line-derived neurotrophic factor; IGF-I, insulin-like growth factor-I; IGF-IR, insulin-like growth factor-I receptor; LY, LY294002; NVP, NVPAAEW541; U, U0126; VEGF, vascular endothelial growth factor.

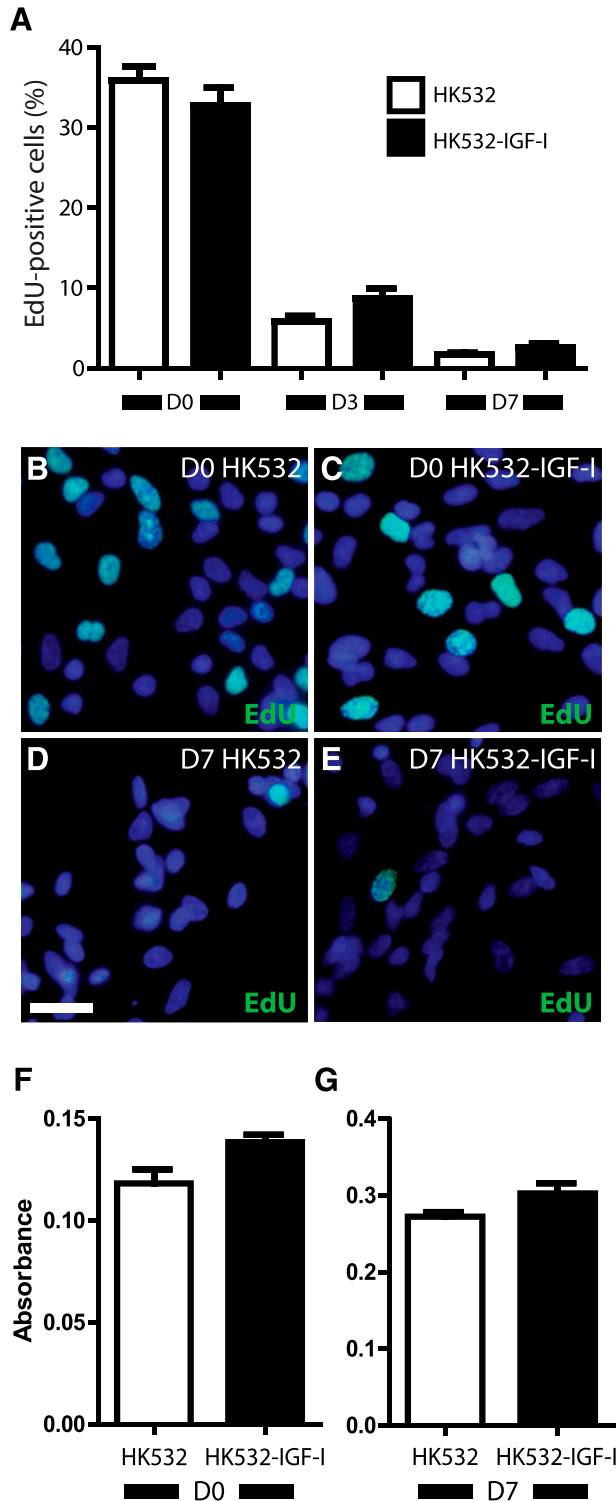


**Figure 2.** Induced insulin-like growth factor-I (IGF-I) expression does not affect HK532 cell proliferation and migration. **(A):** Quantification of the percent of EdU-positive cells at D0, D3, and D7 in HK532 and HK532-IGF-I cultures. **(B–E):** Representative immunocytochemistry images of D0 and D7 HK532 and HK532-IGF-I cells labeled with 4',6-diamidino-2-phenylindole (DAPI) (blue) and EdU (green). **(F–G):** Quantification of absorbance of migrated HK532 and HK532-IGF-I cells at D0 and D7. Data are presented as mean + SD or are representative images of at least three independent experiments. Scale bar = 200  $\mu\text{m}$ . \*,  $p < .05$ . Abbreviations: D0 (D3, D7), day 0 (day 3, day 7); EdU, 5'-ethynyl-2'-deoxyuridine.

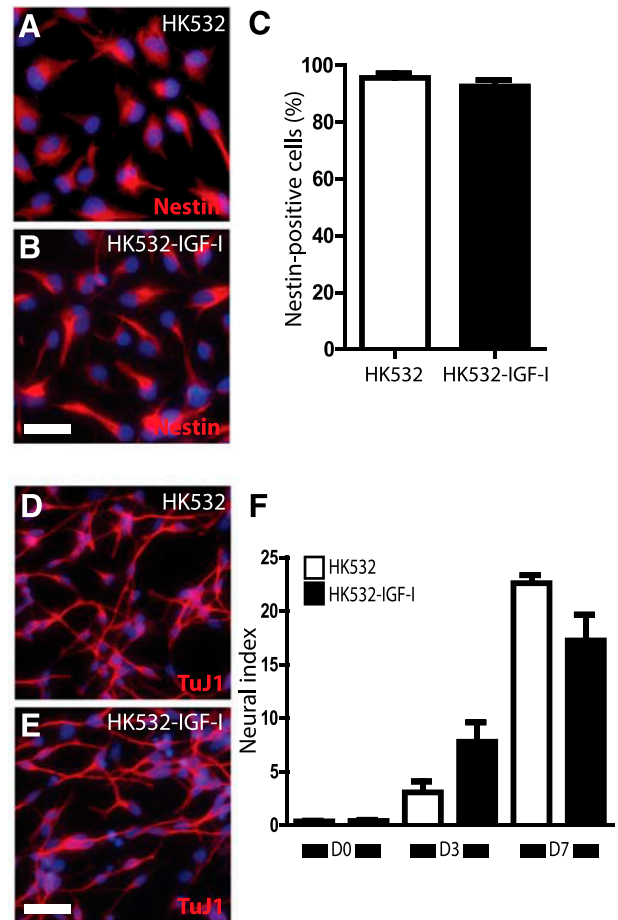


**Figure 3.** Induced insulin-like growth factor-I (IGF-I) expression does not affect maintenance of progenitor status or neurite outgrowth during differentiation. **(A, B):** Representative immunocytochemistry (ICC) image of D0 HK532 and HK532-IGF-I cells labeled with 4',6-diamidino-2-phenylindole (DAPI) (blue) and Nestin (red). **(C):** Quantification of Nestin-positive D0 HK532 and HK532-IGF-I cells. **(D, E):** Representative ICC image of D7 HK532 and HK532-IGF-I cells labeled with DAPI (blue) and TUJ1 (red). **(F):** Quantification of the neural index measurement ( $\mu\text{m}^2$  per cell). Data are presented as mean + SD or are representative images of at least three independent experiments. Scale bar = 200  $\mu\text{m}$ . \*,  $p < .05$ . Abbreviation: D7, day 7.

**IGF-I-Expressing HK532 Cells Retain Neural Differentiation Capacity**

We previously reported that both exogenous and autocrine IGF-I-enhanced spinal NSC neural differentiation [41, 42], and so we next examined the impact of IGF-I on the maintenance of HK532 progenitor status and axonal outgrowth. Approximately 92% and 90% of D0 HK532 and HK532-IGF-I cells were Nestin positive, respectively, indicating that IGF-I expression did not affect the maintenance of progenitor status. IGF-I promotes axonal outgrowth [50, 54, 55], so we also assessed the effect of IGF-I on neurite outgrowth, using our established neural index approach as an early indicator of neuronal differentiation [41, 42, 56]. For both HK532 and HK532-IGF-I cells, the neural index increased between D0 and D7 as the cells differentiated, but we did not observe any significant differences between the cell lines at any time point tested (Fig. 3F). These

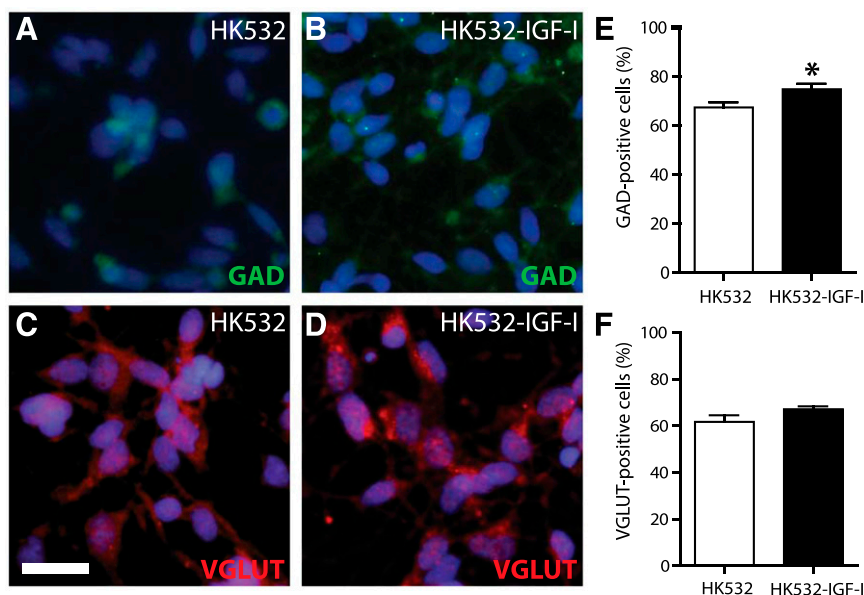


**Figure 4.** Terminal phenotype of HK532 and HK532-IGF-I cells. (A, B): Representative immunocytochemistry (ICC) images of D7 HK532 and HK532-IGF-I cells labeled with 4',6-diamidino-2-phenylindole (DAPI) (blue) and GAD65 (green). (C, D): Representative ICC image of D7 cells labeled with DAPI (blue) and VGLUT (red). (E): Quantification of GAD65-positive gamma-aminobutyric acid (GABA)ergic neurons in HK532 and HK532-IGF-I cells. HK532-IGF-I cells preferentially differentiate into GABAergic neurons (\*,  $p < .05$  vs. HK532). (F): Quantification of VGLUT-positive glutamatergic neurons in HK532 and HK532-IGF-I cells. Data are presented as representative images or mean + SD of at least three independent experiments. Scale bar = 200  $\mu$ m. Abbreviations: D7, day 7; GAD, glutamic acid decarboxylase; VGLUT, vesicular glutamate transporter.

data demonstrate that IGF-I does not affect initial HK532 cell differentiation.

#### GABAergic But Not Glutamatergic Phenotypes Are Increased in HK532-IGF-I Cells

Glutamatergic (VGLUT) and gamma-aminobutyric acid-ergic (GABAergic; GAD65) phenotypes at D0, D3, and D7 were quantified to determine the impact of IGF-I on terminal differentiation. GAD65-positive cells were significantly increased in the HK532-IGF-I cell line compared with the parental HK532 cells, at 74% and 67% of total cells, respectively (Fig. 4A, 4B, 4E). The percentage of VGLUT-positive cells in HK532 (61%) and HK532-IGF-I (67%) cultures were not significantly different (Fig. 4C, 4D, 4F). These data demonstrate that IGF-I increases the number of GABAergic neurons resulting from cell differentiation but has no significant effect on the number of glutamatergic neurons.

#### HK532-IGF-I Are Resistant to $A\beta$ Toxicity and Protect Primary CNs In Vitro

$A\beta$ (1-42) is a commonly used in vitro model of AD-associated toxicity [57]. Significant apoptosis and CC3 activation was observed in primary CNs and both NSC lines when exposed to  $A\beta$  (Fig. 5A). However, apoptosis levels in HK532 and HK532-IGF-I cells were significantly lower than that observed in primary CNs ( $p < .001$ ) (Fig. 5A), and HK532-IGF-I cells displayed increased resistance to  $A\beta$  toxicity compared with parental cells ( $p < .05$ ) (Fig. 5A). Furthermore, after 7 days of differentiation, both cell lines displayed increased resistance to  $A\beta$  toxicity; again, this was significantly increased in HK532-IGF-I cells. Addition of the IGF-IR inhibitor NVP reverted this increased resistance of

HK532-IGF-I cells back to levels of parental cells, indicating that IGF-I production contributes to this enhanced resistance (Fig. 5A). To examine the protective capacity of the modified NSCs,  $A\beta$  toxicity was also assessed in primary CNs indirectly cocultured with HK532 and HK532-IGF-I cells (Fig. 5B–5E). When quantified, apoptosis in CNs, again indicated by CC3 activation, was significantly decreased to below 40% when cocultured with HK532 cells and to below 30%, when cocultured with HK532-IGF-I cells ( $p < .05$ ) (Fig. 5H). These data indicate the HK532-IGF-I cell line is neuroprotective and prevents  $A\beta$ -induced CN death by a paracrine mechanism. Moreover, NVP reversed the additive neuroprotection conferred by HK-532-IGF-I to that of parental HK532 (Fig. 5F–5H), thus indicative of a significant contribution of IGF-I to HK532-IGF-I neuroprotection.

#### HK532-IGF-I Survive Transplantation and Incorporate In Vivo in an AD Mouse Model

We next transplanted HK532-IGF-I cells into APP/PS1 double-transgenic mice, a commonly used model of AD [10, 58–64], to establish the feasibility of preclinical testing. This pilot study enabled optimization of targeting the fimbria fornix of the hippocampus and assessment of transplanted cell survival over time. Targeting accuracy was achieved in all animals injected. Transplanted human cells were detected by IHC for HuNu and DCX at 2 weeks (data not shown) and at 10 weeks post-transplantation (Fig. 6). Grafted cells were evident in the hippocampal regions of both AD (Fig. 6A–6F) and WT animals (Fig. 6G–6L). Costaining of HuNu with DCX, which labels neuronal precursors and is indicative of neurogenesis, suggested that transplanted cortical NSCs were in an early neuronal differentiation phase.

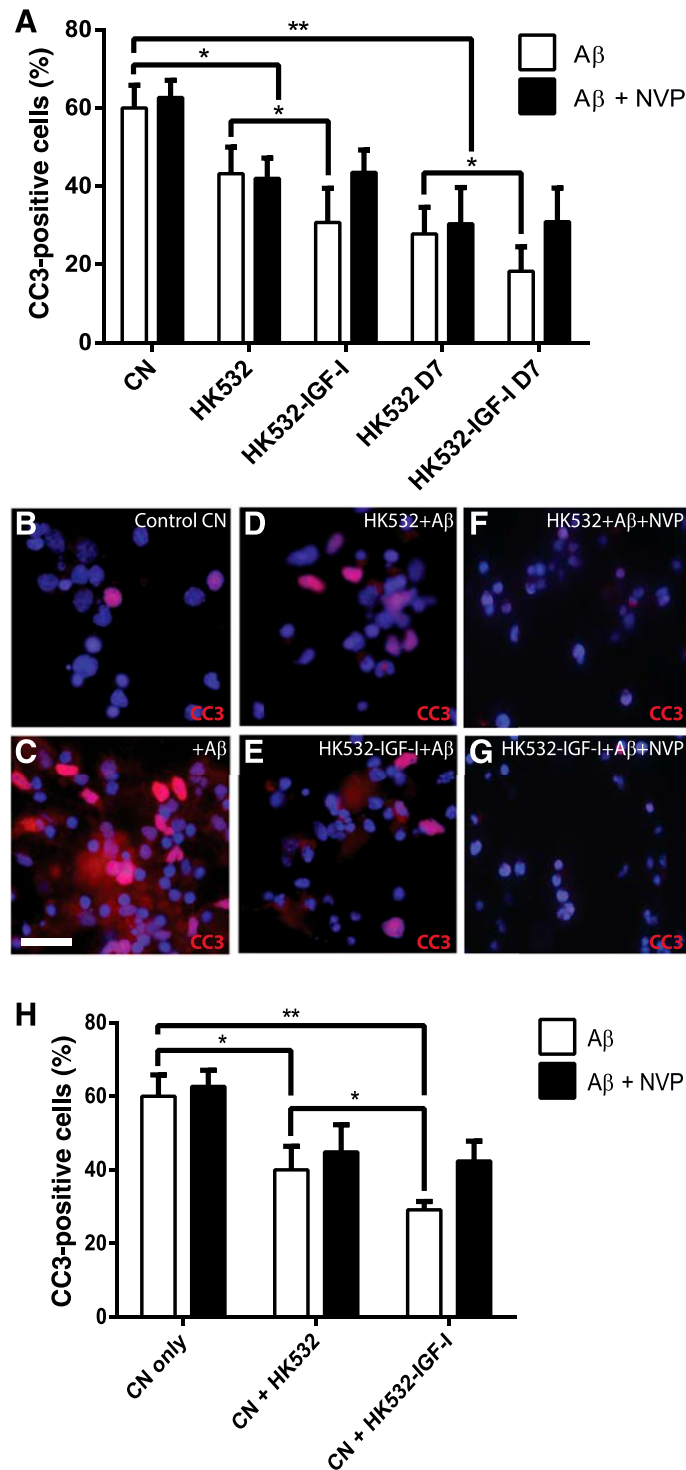


**Figure 5.** HK532-IGF-I cells are neuroprotective in vitro. **(A):** Quantification of apoptosis and cleaved caspase-3 (CC3) activation in response to Aβ toxicity in primary CNs and undifferentiated and differentiated (D7) HK532 and HK532-IGF-I cells. Both HK532 cell lines were more resistant than CNs, and HK532-IGF-I cells displayed significantly increased resistance, which was negated when insulin-like growth factor-I (IGF-I) signaling is blocked by addition of NVP. **(B–G):** Representative immunocytochemistry images of primary CNs labeled with DAPI and CC3, where conditions included **(B)** control CNs with no Aβ treatment, **(C)** CNs with Aβ treatment, **(D)** CNs with Aβ treatment cocultured with HK532 cells, **(E)** CNs with Aβ treatment cocultured with HK532-IGF-I cells, **(F)** CNs with Aβ treatment cocultured with HK532 cells plus NVP, and **(G)** CNs with Aβ treatment cocultured with HK532-IGF-I cells plus NVP. **(H):** Quantification of Aβ-mediated apoptosis and CC3 activation in CN/HK532 cocultures. HK532-IGF-I cells exhibited an increased neuroprotective capacity (\*,  $p < .05$  vs. HK532), which was reversed with addition of NVP. Data are presented as mean + SD or representative images of at least three independent experiments. Scale bar = 200 μm. \*,  $p < .05$ ; \*\*,  $p < .0005$ . Abbreviations: Aβ, amyloid β; CC3, cleaved caspase-3; CN, cortical neuron; NVP, NVP/AEW541.



## DISCUSSION

There is no cure for AD and no means of prevention. Currently approved drug treatments temporarily slow dementia symptoms but ultimately fail to alter the disease course. Despite multitudes of prospective compounds moving through the AD drug development pipeline, little progress has been made and no new treatments have been approved for AD since 2003 [65]. Given the prevalence of AD and an increasingly aging population, we urgently need to identify new therapeutic strategies. We contend that a breakthrough disease modifying treatment for AD must address complex underlying disease pathologies as well as delay or even prevent neuronal damage and synaptic degeneration.

NSC transplantation represents an exciting new approach to treat AD. NSCs have a long-term self-renewal capacity, the potential to differentiate into a number of neural cell types, and the ability to provide an unlimited source of cells for regenerative medicine applications. Transplantation of NSCs improves brain or motor functions after stroke, Parkinson's disease, and amyotrophic lateral sclerosis (ALS) [66–68]. We have previously shown that human spinal NSCs develop neuronal morphologies and form synapses with host neurons in the spinal cord of ALS rats [67]. Furthermore, transplanted stem cells were able to modulate inflammation and significantly reduced astroglial and microglial activation [67]. In AD, cell therapies also have the potential to modify the disease environment by multiple mechanisms, conferring a distinct advantage over single-target drug therapies. Cell transplantation also carries the unique advantage of allowing sustained delivery of peptides or large molecules, without needing to contend with the blood-brain barrier and avoiding systemic side effects. In fact, recent reports indicate that human central nervous system-derived NSCs improve cognition in murine AD models [69, 70], further validating our approach and emphasizing the need to identify the most effective cell type that will provide the most clinical benefit to patients with AD.

In the present study, we engineered a human cortical NSC line to produce increased levels of IGF-I to establish an enhanced and multifaceted cellular therapy for AD. IGF-I is a potent neurotrophic factor that promotes neurogenesis and synaptogenesis and also exerts antiapoptotic and anti-inflammatory effects [30, 31, 38–45]. Given the neuroprotective potential of IGF-I, we hypothesized that an enhanced human NSC line would prove advantageous by providing cell-mediated protection as well as further enriching the diseased environment. In AD, this potentially includes the formation of synaptic contacts with host neurons, modulation of inflammation, and the provision of general neurotrophic support in the brain milieu, in addition to the benefits of IGF-I production, synergistically blocking cell and synapse loss.

Here, we investigated the characteristics and therapeutic potential of an enhanced NSC line, HK532-IGF-I. These cells exhibited a 50-fold increase in IGF-I expression with robust expression maintained throughout early differentiation, consistent with results seen in our previous studies and those of others using a similar approach [42, 71, 72]. Both parental HK532 and HK532-IGF-I cells exhibited normal IGF-IR activation and MAPK/Akt signaling profiles; however, we did observe a diminished responsiveness to exogenous IGF-I stimulation in HK532-IGF-I cells at both time points examined. This is not unexpected, because HK532-IGF-I cells displayed decreased levels of IGF-IR relative

to parental HK532 cells. It is also well documented that continuous IGF-I stimulation results in IGF-I insensitivity, decreased receptor expression, and desensitization of IGF-IR [41, 42]. In line with our previous studies in spinal NSCs, we also see increased IGF-IR expression and signaling after differentiation in both cell lines [42]. HK532 cells produce a number of growth factors, including BDNF, GDNF, and VEGF. The cell secretome remains largely unchanged in modified HK532-IGF-I cells relative to parental cells, with the exception of VEGF, significantly increased levels of which were detected in undifferentiated cells. Such an increase in VEGF secretion may, in fact, augment the neuroprotective impact of HK532-IGF-I cells *in vivo*. Several studies report beneficial neurotrophic effects of cell-mediated VEGF production in AD, which include reducing senile plaques, preventing AD-associated excitotoxicity by decreasing acetylcholinesterase expression and activity (a similar mechanism to AD drug treatments), and providing cognitive benefit *in vivo* [17, 73].

IGF-I impacts multiple cellular behaviors, including proliferation, migration, and differentiation [29–32]. Bearing in mind our goal to develop HK532-IGF-I into a cellular therapy for use in patients, we next confirmed that that autocrine production of IGF-I does not adversely impact cell behavior. No significant differences were found in HK532-IGF-I cell proliferation relative to parental cells at any time point. We also verified that enhanced IGF-I expression does not influence the migratory capacity of HK532-IGF-I cells. These findings are perhaps attributable to the reduced expression of IGF-IR observed in HK532-IGF-I relative to HK532, and indicate that IGF-I does not act as a mitogen for HK532 cells. These data are similar to our previous studies assessing exogenous IGF-I addition or induced IGF-I expression in human spinal NSCs [41, 42], and demonstrate that combining IGF-I with HK532 cells does not promote undesirable propagation. Together, these data form a preliminary safety profile for HK532-IGF-I cells, which will be confirmed by rigorous *in vivo* tumorigenesis studies, as required by the FDA for further preclinical development.

Interestingly, IGF-I modification did not significantly affect the amount of differentiation observed between cell lines. Our previous work on spinal NSCs demonstrated an increase in differentiation with IGF-I [41], suggesting that the effects of IGF-I on neural progenitor differentiation is cell-line specific. We did, however, observe a significant change in the terminal phenotype, where HK532-IGF-I cells yielded significantly increased numbers of GAD65-positive GABAergic neurons. This is therapeutically relevant because diminished function of GABAergic neurons is reported in mouse models and human patients [74, 75]. Thus, an interesting idea to pursue is whether HK532-IGF-I transplantation may provide a source of *de novo* GABAergic neurons to replace those dysregulated in AD and restore critical neurocircuitry in the brain.

The neuroprotective capacity of IGF-I and its ability to prevent apoptosis has been shown in multiple neural cell types, including cortical, motor, and sensory neurons, when subjected to a wide range of stressors [30, 33, 45, 76–79]. Exogenous IGF-I also improves transplant microenvironments and promotes transplanted cell survival under different pathological conditions *in vivo*, including spinal cord injury [78, 80]. To assess the therapeutic impact of HK532-IGF-I, we first examined the susceptibility of our enhanced IGF-I cell line to the AD microenvironment by treating cells with  $A\beta$ , which is neurotoxic to neuronal cell lines *in vitro* [81, 82]. We found significantly reduced

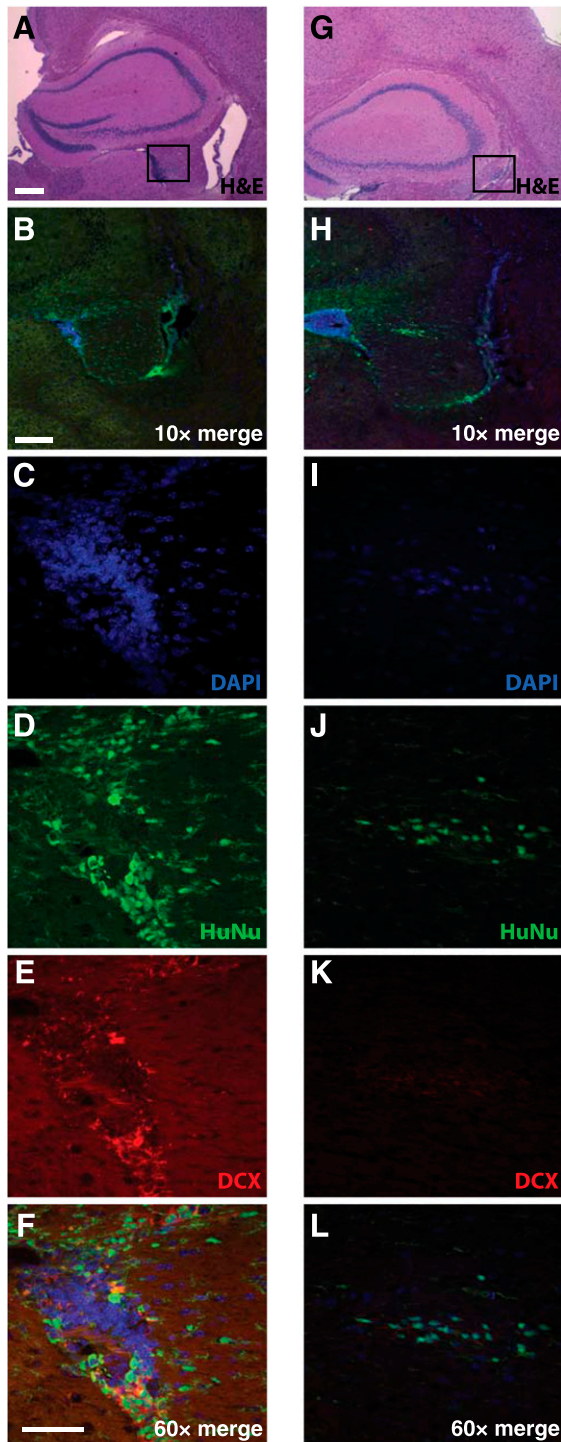


**Figure 6.** HK532-IGF-I cells survive grafting into APP/PS1 mice with Alzheimer's disease (AD) and wild-type (WT) mice. Representative images of HK532-IGF-I cells in the hippocampal area of APP/PS1 AD (A–F) and WT (G–L) mice 10 weeks following transplantation to the fimbria fornix. H&E staining shows the transplanted target area (square) in AD (A) and WT (G) mice. Immunofluorescent DAPI, HuNu, and DCX labeling of human early neural precursor cells in the hippocampal area of AD (B–F) and WT animals (H–L). Data are presented as representative images (A–F: APP/PS1,  $n = 4$ ; G–L: WT,  $n = 4$ ). (A, G): Scale bar = 200  $\mu\text{m}$ . (B, H):  $\times 10$  scale bar = 200  $\mu\text{m}$ . (C–F, I–L):  $\times 60$  scale bar = 50  $\mu\text{m}$ . Abbreviations: DAPI, 4',6-diamidino-2-phenylindole; DCX, Doublecortin; H&E, hematoxylin and eosin; HuNu, human nuclei.

levels of cell death in both undifferentiated and differentiated HK532-IGF-I cells compared with that observed in primary CNs. These data indicate that these cortical NSCs display an increased resistance to AD-related toxicity, supporting their ability to survive following intracranial transplantation, and offer a healthy, more resistant cellular population in the AD brain. We also demonstrated reduced apoptosis of CNs when they are indirectly cocultured with HK532-IGF-I cells. Importantly, this enhanced protection is attributed to increased levels of IGF-I, as evidenced by an increased protective capacity of HK532-IGF-I cells relative to HK532 cells and reversal of this effect when IGF-I signaling is inhibited. This is supported by our previous findings demonstrating that IGF-I expression increased resistance of spinal cord NSCs to cellular insults [41, 42]. Together, these data indicate that IGF-I will provide enhanced protection in AD, advocating the potential therapeutic efficacy of HK532-IGF-I. Furthermore, in the context of the hippocampus, we predict that in addition to preventing cell death, HK532-IGF-I will promote neurogenesis and synaptogenesis in the hippocampus via IGF-I-mediated signaling [40, 83], which will be addressed in our future preclinical studies.

Finally, we tested the feasibility of HK532-IGF-I transplantation into the AD brain using the APP/PS1 transgenic mouse. APP/PS1 mice have been used extensively as a preclinical model of AD [58–64]. Here, we report successful cellular transplantation into the murine fimbria fornix, a major projection pathway connecting the hippocampus to cortical and subcortical brain structures. Targeting this area for cell transplantation will provide a de novo tissue source as well as trophic support, and, importantly, impacting this target area has the potential to rescue memory and learning deficits in AD. Our preliminary data demonstrate successful targeting of HK532-IGF-I cells into the fimbria fornix of the hippocampus in the AD brain. Grafts were detected 2 weeks and 10 weeks posttransplantation by HuNu staining, verifying survival of human cells in the AD brain for a clinically relevant period of time. We saw no difference in cell graft size between WT and AD animals. In addition, HuNu-positive cells expressed DCX, a marker of neurogenesis. DCX expression is specific to newly generated healthy neurons [84], and indicated that the transplanted cells were differentiating into neural cell types *in vivo*. Together, these data provide a platform for future, large-scale, preclinical studies in murine models of AD to assess the therapeutic benefit of cellular therapy in modifying deficits in behavior, memory, and learning.

#### CONCLUSION

NSC transplantation offers a novel and potentially transformative approach to treating neurodegenerative disease. The safety of such cell therapies is now established in several clinical trials, including our own trial in patients with ALS [85–87]. To progress to similar trials in patients with AD, it is critical that NSC lines providing the greatest efficacy be identified; this prompted us to generate the enhanced NSC line, HK532-IGF-I. We report that autocrine IGF-I production does not impact normal cellular functions, including proliferation, migration, or maintenance of progenitor status, thus maintaining the potential safety profile of this cell line for future clinical application. HK532-IGF-I cells display a significantly enhanced neuroprotective capacity *in vitro* and survive long term *in vivo* after transplantation into the murine AD brain,

confirming the feasibility of our approach. We predict that in AD, HK532-IGF-I cells will provide additional environmental enrichment through IGF-I production, secondary to beneficial effects on synaptogenesis and inflammation, as observed in the spinal cord of ALS models. Additionally, HK532-IGF-I cells preferentially differentiate into GABAergic neurons, a population selectively lost in AD, and produce increased levels of VEGF, further validating this cell line as a suitable candidate for cell transplantation. Future, large-scale small-animal studies are necessary to establish preclinical efficacy in models of AD. Overall, our findings support further development of IGF-I-producing NSCs as a safe and clinically translatable cellular therapy for patients with AD.

#### ACKNOWLEDGMENTS

We thank Dr. Mike Hefferan, Neuralstem, Inc.; Dr. Sang Su Oh, University of Michigan; and Dr. Bhumsoo Kim, University of Michigan, for technical assistance. This research was supported by the A. Alfred Taubman Medical Research Institute, the Program for Neurology Research & Discovery, and the Robert E. Nelderlander Sr. Program for Alzheimer's Research. K.S.C. and O.N.K. are currently supported by the University of Michigan Clinician Scientist Training Programs (Grants NINDS R25NS089450 and NIH T32NS07222).

#### AUTHOR CONTRIBUTIONS

L.M.M.: conception and design, collection and assembly of data, data analysis and interpretation, manuscript writing, final approval of manuscript; E.S.: collection and assembly of data, manuscript writing, final approval of manuscript. J.S.L.: conception and design, collection and assembly of data, data analysis and interpretation, final approval of manuscript; O.N.K. and K.S.C.: data analysis and interpretation, manuscript writing, final approval of manuscript; E.S.B.: collection and/or assembly of data, data analysis and interpretation, final approval of manuscript; C.M.P.: collection and/or assembly of data, final approval of manuscript; T.H. and K.J.: provision of study material, final approval of manuscript; S.A.S.: manuscript writing, final approval of manuscript; E.L.F.: conception and design, financial support, final approval of manuscript.

#### DISCLOSURE OF POTENTIAL CONFLICTS OF INTEREST

T.H. is an employee of Neuralstem, Inc. K.J. is an employee of Neuralstem, Inc., is a compensated patent holder of neural stem cells reported in this study, and has compensated stock options. E.L.F. is an uncompensated consultant for Neuralstem, Inc. The other authors indicated no potential conflicts of interest.

#### REFERENCES

- Thies W, Bleiler L. 2013 Alzheimer's disease facts and figures. *Alzheimers Dement* 2013;9:208–245.
- Katzman R. Alzheimer's disease. *N Engl J Med* 1986;314:964–973.
- LaFerla FM, Tinkle BT, Bieberich CJ et al. The Alzheimer's A beta peptide induces neurodegeneration and apoptotic cell death in transgenic mice. *Nat Genet* 1995; 9:21–30.
- Selkoe DJ. Alzheimer's disease is a synaptic failure. *Science* 2002;298:789–791.
- Castellani RJ, Rolston RK, Smith MA. Alzheimer disease. *Dis Mon* 2010;56:484–546.
- Eckman CB, Eckman EA. An update on the amyloid hypothesis. *Neurol Clin* 2007;25: 669–682, vi [vi.].
- Howard R, McShane R, Lindsay J et al. Donepezil and memantine for moderate-to-severe Alzheimer's disease. *N Engl J Med* 2012;366:893–903.
- Hyde C, Peters J, Bond M et al. Evolution of the evidence on the effectiveness and cost-effectiveness of acetylcholinesterase inhibitors and memantine for Alzheimer's disease: Systematic review and economic model. *Age Ageing* 2013;42:14–20.
- Lunn JS, Sakowski SA, Hur J et al. Stem cell technology for neurodegenerative diseases. *Ann Neurol* 2011;70:353–361.
- Weiner MW. Dementia in 2012: Further insights into Alzheimer disease pathogenesis. *Nat Rev Neurol* 2013;9:65–66.
- Small SA, Schobel SA, Buxton RB et al. A pathophysiological framework of hippocampal dysfunction in ageing and disease. *Nat Rev Neurosci* 2011;12:585–601.
- Blurton-Jones M, Kitazawa M, Martinez-Coria H et al. Neural stem cells improve cognition via BDNF in a transgenic model of Alzheimer disease. *Proc Natl Acad Sci USA* 2009;106: 13594–13599.
- Hampton DW, Webber DJ, Bilican B et al. Cell-mediated neuroprotection in a mouse model of human tauopathy. *J Neurosci* 2010; 30:9973–9983.
- Moghadam FH, Alaie H, Karbalaie K et al. Transplantation of primed or unprimed mouse embryonic stem cell-derived neural precursor cells improves cognitive function in Alzheimerian rats. *Differentiation* 2009; 78:59–68.
- Wang Q, Matsumoto Y, Shindo T et al. Neural stem cells transplantation in cortex in a mouse model of Alzheimer's disease. *J Med Invest* 2006;53:61–69.
- Zhang JQ, Yu XB, Ma BF et al. Neural differentiation of embryonic stem cells induced by conditioned medium from neural stem cell. *Neuroreport* 2006;17:981–986.
- Garcia KO, Ornellas FL, Martin PK et al. Therapeutic effects of the transplantation of VEGF overexpressing bone marrow mesenchymal stem cells in the hippocampus of murine model of Alzheimer's disease. *Front Aging Neurosci* 2014;6:30.
- Lee HJ, Lee JK, Lee H et al. Human umbilical cord blood-derived mesenchymal stem cells improve neuropathology and cognitive impairment in an Alzheimer's disease mouse model through modulation of neuroinflammation. *Neurobiol Aging* 2012;33:588–602.
- Lee JK, Jin HK, Endo S et al. Intracerebral transplantation of bone marrow-derived mesenchymal stem cells reduces amyloid-beta deposition and rescues memory deficits in Alzheimer's disease mice by modulation of immune responses. *STEM CELLS* 2010;28:329–343.
- Lindvall O, Kokaia Z. Stem cells for the treatment of neurological disorders. *Nature* 2006;441:1094–1096.
- Martinez-Serrano A, Björklund A. Protection of the neostriatum against excitotoxic damage by neurotrophin-producing, genetically modified neural stem cells. *J Neurosci* 1996;16:4604–4616.
- Wu S, Sasaki A, Yoshimoto R et al. Neural stem cells improve learning and memory in rats with Alzheimer's disease. *Pathobiology* 2008; 75:186–194.
- Nayak MS, Kim YS, Goldman M et al. Cellular therapies in motor neuron diseases. *Biochim Biophys Acta* 2006;1762:1128–1138.
- Suzuki M, Svendsen CN. Combining growth factor and stem cell therapy for amyotrophic lateral sclerosis. *Trends Neurosci* 2008; 31:192–198.
- Hedlund E, Hefferan MP, Marsala M et al. Cell therapy and stem cells in animal models of motor neuron disorders. *Eur J Neurosci* 2007; 26:1721–1737.
- Lunn JS, Hefferan MP, Marsala M et al. Stem cells: Comprehensive treatments for amyotrophic lateral sclerosis in conjunction with growth factor delivery. *Growth Factors* 2009;27:133–140.
- Anlar B, Sullivan KA, Feldman EL. Insulin-like growth factor-I and central nervous system development. *Horm Metab Res* 1999;31: 120–125.
- Russo VC, Gluckman PD, Feldman EL et al. The insulin-like growth factor system and its pleiotropic functions in brain. *Endocr Rev* 2005;26:916–943.
- Alagappan D, Ziegler AN, Chidambaram S et al. Insulin-like growth factor

receptor signaling is necessary for epidermal growth factor mediated proliferation of SVZ neural precursors in vitro following neonatal hypoxia-ischemia. *Front Neurol* 2014; 5:79.

30 Hodge RD, D'Ercole AJ, O'Kusky JR. Insulin-like growth factor-I (IGF-I) inhibits neuronal apoptosis in the developing cerebral cortex in vivo. *Int J Dev Neurosci* 2007;25: 233–241.

31 Zaka M, Rafi MA, Rao HZ et al. Insulin-like growth factor-1 provides protection against psychosine-induced apoptosis in cultured mouse oligodendrocyte progenitor cells using primarily the PI3K/Akt pathway. *Mol Cell Neurosci* 2005;30:398–407.

32 Zhang X, Lin M, van Golen KL et al. Multiple signaling pathways are activated during insulin-like growth factor-I (IGF-I) stimulated breast cancer cell migration. *Breast Cancer Res Treat* 2005;93:159–168.

33 Vincent AM, Consilvio C, Feldman EL. IGF-I-mediated protection of motor neurons in a cell culture model of ALS. *Endocrine Society Abstracts* 2003;3–316.

34 Vincent AM, Feldman EL, Song DK et al. Adeno-associated viral-mediated insulin-like growth factor delivery protects motor neurons in vitro. *Neuromolecular Med* 2004;6: 79–85.

35 Miltiadou P, Stamatakis A, Koutsoudaki PN et al. IGF-I ameliorates hippocampal neurodegeneration and protects against cognitive deficits in an animal model of temporal lobe epilepsy. *Exp Neurol* 2011;231:223–235.

36 Pang Y, Zheng B, Fan LW et al. IGF-1 protects oligodendrocyte progenitors against TNF $\alpha$ -induced damage by activation of PI3K/Akt and interruption of the mitochondrial apoptotic pathway. *Glia* 2007;55:1099–1107.

37 Delaney CL, Cheng HL, Feldman EL. Insulin-like growth factor-I prevents caspase-mediated apoptosis in Schwann cells. *J Neurobiol* 1999;41:540–548.

38 Cheng CM, Mervis RF, Niu SL et al. Insulin-like growth factor 1 is essential for normal dendritic growth. *J Neurosci Res* 2003;73:1–9.

39 Gandhi D et al. IGF-I rescues neurons from hyperglycemic, hyperosmotic injury. In: Hotta N, Greene DA, Ward JD, Sima AAF, Boulton AJM, eds. *Diabetic Neuropathy: New Concepts and Insights*. Amsterdam, The Netherlands: Elsevier Science B.V., 1995: 183–189.

40 Hung KS, Tsai SH, Lee TC et al. Gene transfer of insulin-like growth factor-I providing neuroprotection after spinal cord injury in rats. *J Neurosurg Spine* 2007;6: 35–46.

41 Lunn JS, Pacut C, Backus C et al. The pleiotropic effects of insulin-like growth factor-I on human spinal cord neural progenitor cells. *Stem Cells Dev* 2010;19:1983–1993.

42 Lunn JS, Sakowski SA, McGinley LM et al. Autocrine production of IGF-I increases stem cell-mediated neuroprotection. *STEM CELLS* 2015;33:1480–1489.

43 Niblock MM, Brunso-Bechtold JK, Riddle DR. Insulin-like growth factor I stimulates dendritic growth in primary somatosensory cortex. *J Neurosci* 2000;20:4165–4176.

44 Stewart CEH, Rotwein P. Growth, differentiation, and survival: Multiple physiological functions for insulin-like growth factors. *Physiol Rev* 1996;76:1005–1026.

45 Sullivan KA, Kim B, Russell JW, Feldman EL. IGF-I in neuronal differentiation and neuroprotection. In: Müller EE, ed. *IGFs in the Nervous System*. Milan, Italy: Springer-Verlag Italia Srl, 1998:28–46.

46 Harada N, Zhao J, Kurihara H et al. Resveratrol improves cognitive function in mice by increasing production of insulin-like growth factor-I in the hippocampus. *J Nutr Biochem* 2011;22:1150–1159.

47 Johe KK, Hazel TG, Muller T et al. Single factors direct the differentiation of stem cells from the fetal and adult central nervous system. *Genes Dev* 1996;10:3129–3140.

48 Xu L, Ryugo DK, Pongstaporn T et al. Human neural stem cell grafts in the spinal cord of SOD1 transgenic rats: Differentiation and structural integration into the segmental motor circuitry. *J Comp Neurol* 2009;514: 297–309.

49 Chia VM, Quraishi SM, Graubard BI et al. Insulin-like growth factor 1, insulin-like growth factor-binding protein 3, and testicular germ-cell tumor risk. *Am J Epidemiol* 2008;167: 1438–1445.

50 Kim B et al. Insulin-like growth factor-I-mediated neurite outgrowth in vitro requires mitogen-activated protein kinase activation. *J Biol Chem* 1997;272:21268–21273.

51 Lunn JS, Pacut C, Stern E et al. Intraspinal transplantation of neurogenin-expressing stem cells generates spinal cord neural progenitors. *Neurobiol Dis* 2012;46:59–68.

52 Kim B, Sullivan KA, Backus C et al. Cortical neurons develop insulin resistance and blunted Akt signaling: A potential mechanism contributing to enhanced ischemic injury in diabetes. *Antioxid Redox Signal* 2011;14: 1829–1839.

53 Shi B, Ding J, Liu Y et al. ERK1/2 pathway-mediated differentiation of IGF-1-transfected spinal cord-derived neural stem cells into oligodendrocytes. *PLoS One* 2014; 9:e106038.

54 Leventhal PS, Shelden EA, Kim B et al. Tyrosine phosphorylation of paxillin and focal adhesion kinase during insulin-like growth factor-I-stimulated lamellipodial advance. *J Biol Chem* 1997;272:5214–5218.

55 Laurino L, Wang XX, de la Houssaye BA et al. PI3K activation by IGF-1 is essential for the regulation of membrane expansion at the nerve growth cone. *J Cell Sci* 2005;118:3653–3662.

56 Kim SJ, Son TG, Kim K et al. Interferon-gamma promotes differentiation of neural progenitor cells via the JNK pathway. *Neurochem Res* 2007;32:1399–1406.

57 Bruce AJ, Malfroy B, Baudry M. beta-Amyloid toxicity in organotypic hippocampal cultures: protection by EUK-8, a synthetic catalytic free radical scavenger. *Proc Natl Acad Sci USA* 1996;93:2312–2316.

58 Cao D, Lu H, Lewis TL et al. Intake of sucrose-sweetened water induces insulin resistance and exacerbates memory deficits and amyloidosis in a transgenic mouse model of Alzheimer disease. *J Biol Chem* 2007;282: 36275–36282.

59 Cheng S, Cao D, Hottman DA et al. Farnesyltransferase haploinsufficiency reduces neuropathology and rescues cognitive function in a mouse model of Alzheimer disease. *J Biol Chem* 2013;288:35952–35960.

60 Cramer PE, Cirrito JR, Wesson DW et al. ApoE-directed therapeutics rapidly clear  $\beta$ -amyloid and reverse deficits in AD mouse models. *Science* 2012;335:1503–1506.

61 Gimbel DA, Nygaard HB, Coffey EE et al. Memory impairment in transgenic Alzheimer mice requires cellular prion protein. *J Neurosci* 2010;30:6367–6374.

62 Lewis TL, Cao D, Lu H et al. Overexpression of human apolipoprotein A-I preserves cognitive function and attenuates neuroinflammation and cerebral amyloid angiopathy in a mouse model of Alzheimer disease. *J Biol Chem* 2010;285:36958–36968.

63 Park JH, Widi GA, Gimbel DA et al. Subcutaneous Nogo receptor removes brain amyloid-beta and improves spatial memory in Alzheimer's transgenic mice. *J Neurosci* 2006; 26:13279–13286.

64 Yang H, Yang H, Xie Z et al. Systemic transplantation of human umbilical cord derived mesenchymal stem cells-educated T regulatory cells improved the impaired cognition in A $\beta$ PPsw/PS1dE9 transgenic mice. *PLoS One* 2013;8:e69129.

65 Cummings JL, Morstorf T, Zhong K. Alzheimer's disease drug-development pipeline: Few candidates, frequent failures. *Alzheimers Res Ther* 2014;6:37.

66 Ebert AD, Beres AJ, Barber AE et al. Human neural progenitor cells overexpressing IGF-1 protect dopamine neurons and restore function in a rat model of Parkinson's disease. *Exp Neurol* 2008;209:213–223.

67 Hefferan MP, Galik J, Kakinohana O et al. Human neural stem cell replacement therapy for amyotrophic lateral sclerosis by spinal transplantation. *PLoS One* 2012;7: e42614.

68 Park KI, Himes BT, Stieg PE et al. Neural stem cells may be uniquely suited for combined gene therapy and cell replacement: Evidence from engraftment of Neurotrophin-3-expressing stem cells in hypoxic-ischemic brain injury. *Exp Neurol* 2006;199:179–190.

69 Ager RR, Davis JL, Agazaryan A. et al. Human neural stem cells improve cognition and promote synaptic growth in two complementary transgenic models of Alzheimer's disease and neuronal loss. *Hippocampus* 2015;25: 813–826.

70 Lee IS, Jung K, Kim IS et al. Human neural stem cells alleviate Alzheimer-like pathology in a mouse model. *Mol Neurodegener* 2015;10: 38.

71 Kouroupi G, Lavdas AA, Gaitanou M et al. Lentivirus-mediated expression of insulin-like growth factor-I promotes neural stem/precursor cell proliferation and enhances their potential to generate neurons. *J Neurochem* 2010;115: 460–474.

72 McGinley L, McMahon J, Strappe P et al. Lentiviral vector mediated modification of mesenchymal stem cells & enhanced survival in an in vitro model of ischaemia. *Stem Cell Res Ther* 2011;2:12.

**73** Antequera D, Portero A, Bolos M et al. Encapsulated VEGF-secreting cells enhance proliferation of neuronal progenitors in the hippocampus of A $\beta$ PP/PS1 mice. *J Alzheimers Dis* 2012;29:187–200.

**74** Loreth D, Ozmen L, Revel FG et al. Selective degeneration of septal and hippocampal GABAergic neurons in a mouse model of amyloidosis and tauopathy. *Neurobiol Dis* 2012; 47:1–12.

**75** Schwab C, Yu S, Wong W et al. GAD65, GAD67, and GABAT immunostaining in human brain and apparent GAD65 loss in Alzheimer's disease. *J Alzheimers Dis* 2013; 33:1073–1088.

**76** Arroba AI, Wallace D, Mackey A et al. IGF-I maintains calpastatin expression and attenuates apoptosis in several models of photoreceptor cell death. *Eur J Neurosci* 2009;30: 975–986.

**77** Brywe KG, Mallard C, Gustavsson M et al. IGF-I neuroprotection in the immature brain after hypoxia-ischemia, involvement

of Akt and GSK3 $\beta$ ? *Eur J Neurosci* 2005; 21:1489–1502.

**78** Kooyman R. Regulation of apoptosis by insulin-like growth factor (IGF)-I. *Cytokine Growth Factor Rev* 2006;17:305–323.

**79** Leininger GM, Backus C, Uhler MD et al. Phosphatidylinositol 3-kinase and Akt effectors mediate insulin-like growth factor-I neuroprotection in dorsal root ganglia neurons. *FASEB J* 2004;18:1544–1546.

**80** Yanagiuchi A, Miyake H, Nomi M et al. Modulation of the microenvironment by growth factors regulates the in vivo growth of skeletal myoblasts. *BJU Int* 2009;103: 1569–1573.

**81** Pike CJ, Burdick D, Walencewicz AJ et al. Neurodegeneration induced by beta-amyloid peptides in vitro: The role of peptide assembly state. *J Neurosci* 1993;13:1676–1687.

**82** Kowall NW, Beal MF, Busciglio J et al. An in vivo model for the neurodegenerative effects of beta amyloid and protection by substance P. *Proc Natl Acad Sci USA* 1991; 88:7247–7251.

**83** Aberg MA, Aberg ND, Hedbäck H et al. Peripheral infusion of IGF-I selectively induces neurogenesis in the adult rat hippocampus. *J Neurosci* 2000;20:2896–2903.

**84** Rao MS, Shetty AK. Efficacy of doublecortin as a marker to analyse the absolute number and dendritic growth of newly generated neurons in the adult dentate gyrus. *Eur J Neurosci* 2004;19:234–246.

**85** Feldman EL, Boulis NM, Hur J et al. Intraspinal neural stem cell transplantation in amyotrophic lateral sclerosis: Phase 1 trial outcomes. *Ann Neurol* 2014;75: 363–373.

**86** Gupta N, Henry RG, Strober J et al. Neural stem cell engraftment and myelination in the human brain. *Sci Transl Med* 2012;4: 155ra137.

**87** Selden NR, Al-Uzri A, Huhn SL et al. Central nervous system stem cell transplantation for children with neuronal ceroid lipofuscinosis. *J Neurosurg Pediatr* 2013;11: 643–652.